

# Radon-220 exhalation methodology and temporal variation in a HBRA, Fen complex

Hallvard Haanes\*<sup>†</sup> and Jostein Hoftuft<sup>†</sup>

Norwegian Radiation and Nuclear Safety Authority, Østerås, Norway

## Abstract

Radon and its progeny are major contributors to dose to the public. In high background radiation areas (HBRAs), the risk is increased. In the Fen igneous complex, Norway, significant outdoor levels of radon-220 ( $^{220}\text{Rn}$ ) have been observed and exhalation from the ground is a contributor. Such exhalation depends on many factors, including levels of radon-progenitors in the ground. Temporal variation in  $^{220}\text{Rn}$  exhalation rates is affected by weather parameters. We show large  $^{220}\text{Rn}$  exhalation rates at Fen complex and assess temporal variation, which is explained by weather parameters, especially by wind. Exhalation rates are calculated from measurement series in an exhalation container using different phases of accumulation. We find a bias depending on whether the linear phase of increase or the subsequent threshold phase is used, and show it is affected by whether air is sampled from the side or top valve of the container. However, in areas where progenitor levels in the ground are low, assessment of the linear phase may not be possible due to required period of measurement intervals.

Keywords: *exhalation rate; weather parameters; radon-220*

To access the Supplementary material, please visit the article landing page

**R**adon-222 ( $^{222}\text{Rn}$ ) and radon-220 ( $^{220}\text{Rn}$ ) are important for dose to the public and workers (1, 2). In high-background radiation areas (HBRAs), the health risk is increased (3, 4). In the Fen igneous complex (Norway), the levels of  $^{226}\text{Ra}$  and  $^{232}\text{Th}$  range up to 1,400 Bq kg<sup>-1</sup> and 12,000 Bq kg<sup>-1</sup>, respectively, in bedrock (5), and up to 380 Bq kg<sup>-1</sup> and 15,500 Bq kg<sup>-1</sup> in soil (6). Outdoor levels of  $^{222}\text{Rn}$  and  $^{220}\text{Rn}$  are as high as 300 and 5,700 Bq/m<sup>3</sup>, respectively (7), due to chimney ventilation from Fen legacy iron mines (8) and soil exhalation.

Radon soil exhalation depends on many factors, namely, soil concentration of its progenitors, permeability, grain size, porosity and humidity (9–11), and weather-parameters like atmospheric temperature, pressure, wind and precipitation (9, 12). Exhalation estimates have often been made by the sealed-can technique (13–16), using alpha track detectors integrating over time. Recent studies use containers, pressure equalisation and *in-situ* measurements (17–19) to assess accumulation of Rn gas during a phase of linear increase before reaching a threshold (Fig. 1a). An estimate of the exhalation rate can be made from the slope of the linear increase phase (ISO 11665-7), from the threshold phase or from exponential

fitting (18). Compared to the time needed to reach the threshold phase, using only the linear phase allows many more exhalation estimates and better assessment of temporal variation. For  $^{220}\text{Rn}$  (half-life of 55.8 s), it may be important to include the reference measurement in the linear phase to attain enough measurements.

We assess  $^{222}\text{Rn}$  and, more comprehensively,  $^{220}\text{Rn}$  exhalation along with its temporal variation and affecting factors in the HBRA Fen complex. We optimise methodology and compare exhalation rates when using measurements from different phases of accumulation.

## Methods

This study location was in the redrock part of the Fen complex (59.2743138N, 9.30713464E). Here, levels in soil range from 65 to 272 Bq kg<sup>-1</sup> for  $^{226}\text{Ra}$  and from 5,100 to 11,500 Bq kg<sup>-1</sup> for  $^{232}\text{Th}$  (6), and at one nearby point, pH is 6.9, the proportion of organic matter is 0.20, whilst sand, silt and clay have the proportions of 0.33, 0.53 and 0.14, respectively (20). A metal exhalation container from SARAD<sup>®</sup> (15 × 50 × 50 cm) minimising sun heating was used. Before placement, litter was removed, and a cut was made in the soil for the circumference of the container

<sup>†</sup>Equal contributions in authorship.

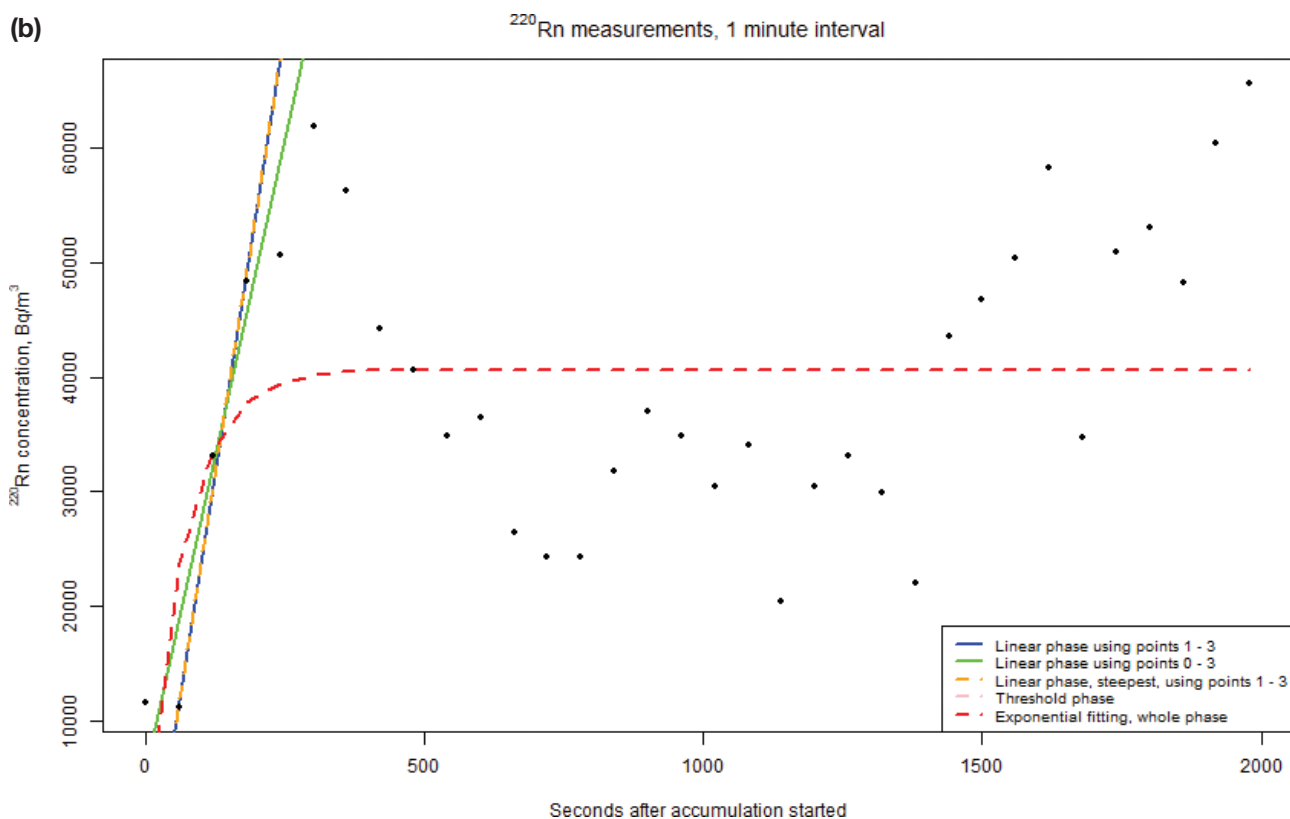
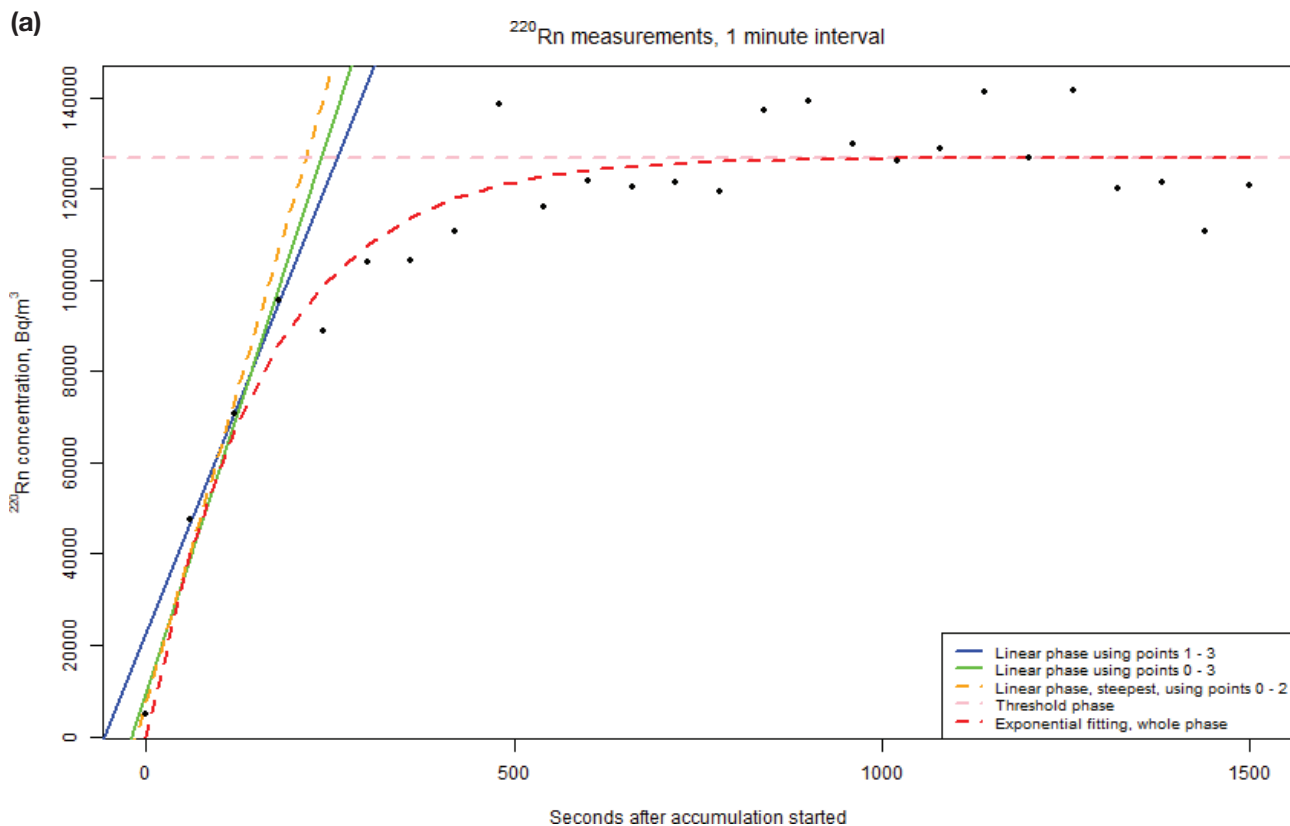


*Fig. 1.* Rn concentration during the linear increase phase and the threshold phase of  $^{220}\text{Rn}$  and  $^{222}\text{Rn}$  accumulation in an exhalation container from ideal (a and c) and non-ideal data (b and d). For b), note the shift in threshold, making such data not suitable for threshold and exponential fitting methods.

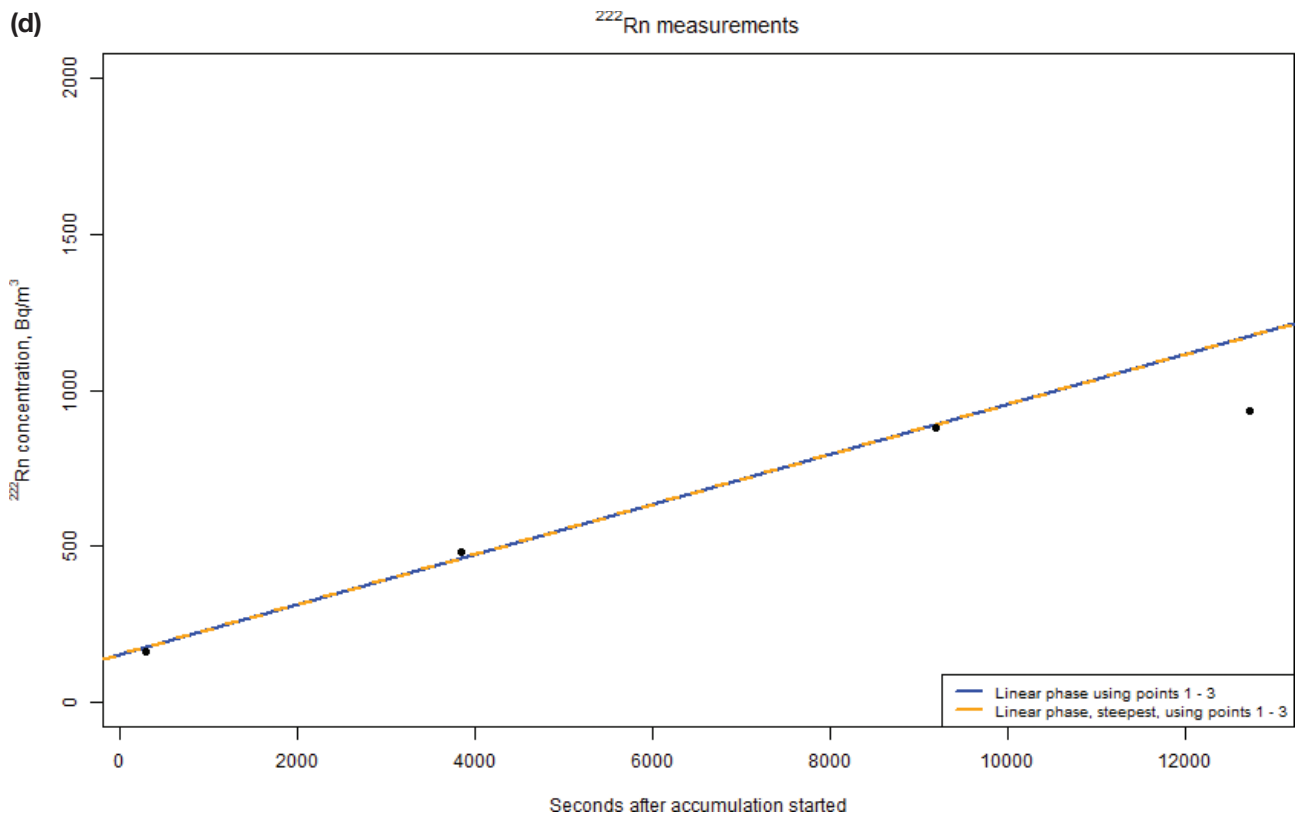
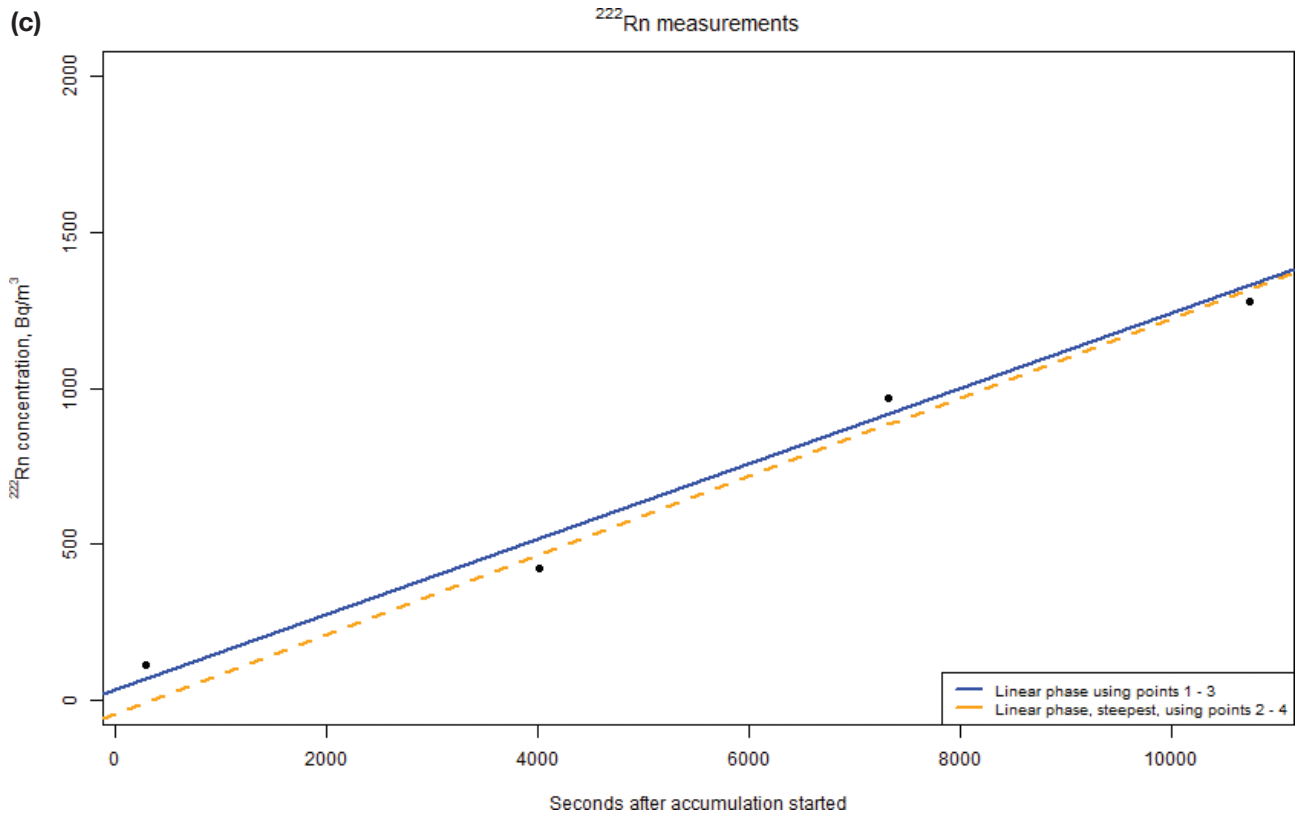


*Fig. 1. (Continued)* Rn concentration during the linear increase phase and the threshold phase of  $^{220}\text{Rn}$  and  $^{222}\text{Rn}$  accumulation in an exhalation container from ideal (a and c) and non-ideal data (b and d). For b), note the shift in threshold, making such data not suitable for threshold and exponential fitting methods.

edge to minimise leakage. Soil was applied along the container. SARAD® EQF 3220, a semi-conductor instrument, was used for  $^{220}\text{Rn}$  measurements, with uncertainty ( $2\sigma$ ) ranging 3–66%. SARAD® RTM1688-2 was used for  $^{222}\text{Rn}$  measurements, with uncertainty ( $2\sigma$ ) ranging 22–110%.

Before placement, a reference measurement was made 5 cm above ground at the height of the side valve, representing the activity concentration before build-up, using 15 and 30-min measurement periods for  $^{220}\text{Rn}$  and  $^{222}\text{Rn}$ , respectively. Tubes were connected to the two valves of the container, in a closed loop circulated by the instrument, using the side valve as outlet in 2021 and 2022, but the top valve at 15 cm height as outlet in 2023. The use of the top valve is according to the ISO. For each exhalation rate estimate, a series of subsequent measurements of air sampled from the outlet were made to assess accumulation of Rn during both the linear and threshold phase (Fig. 1). Due to the high levels of  $^{220}\text{Rn}$ , these series used 1-min period measurements, whilst a 30-min period was required for  $^{222}\text{Rn}$ . We purged the instrument after each series and re-placed the container for each new exhalation rate measurement series. For method optimisation and corrections due to decay, see Supplementary material. For  $^{220}\text{Rn}$ , we performed 41 measurement series, whilst only eight (one per day) were possible for  $^{222}\text{Rn}$  due to its half-life. It takes a lot of time to gain each exhalation rate estimate, and we were limited by time and resources. To assess the exhalation rate measurement series, six different methods (below) using measurements from different phases of accumulation were used to calculate the exhalation rate,  $\Phi$  ( $\text{Bq m}^{-2} \text{ s}^{-1}$ ). In all methods, we assume no leakage, and we assess net exhalation assuming negligible diffusion back into soil:  $\lambda_L = \lambda_B = 0$  ( $\text{s}^{-1}$ ). All deductions and uncertainty equations are in the supplementary material. We simulate a sealed-can using alpha track detectors integrating an average value of  $^{220}\text{Rn}$  over time (exposure  $E$  ( $\text{Bq m}^{-3} \text{ s}$ )) to estimate exhalation (21). This simulation uses datapoints from both phases of accumulation to calculate the exhalation rate:

$$\Phi = \frac{E \cdot V \cdot \lambda_{th}}{S \cdot T_{eff}} \quad \text{Eq. 1}$$

where  $\lambda_{th} = (12.42 \pm 0.07) \cdot 10^{-3} \text{ s}^{-1}$  is the decay constant for  $^{220}\text{Rn}$ ,  $T_{eff} = T + \frac{1}{\lambda_{th}}(e^{-\lambda_{th}T} - 1)$  (s) and  $T$  (s) is the duration of the measurement.

We also assess only the threshold phase of measurement series to estimate  $^{220}\text{Rn}$  exhalation (18, 22–24):

$$\Phi = \frac{C_{lim} \cdot V \cdot \lambda}{S} \quad \text{Eq. 2}$$

where  $\lambda = \lambda_i + \lambda_L + \lambda_B$  ( $\text{s}^{-1}$ ),  $\lambda_i$  ( $\text{s}^{-1}$ ) is the decay constant of the radon isotope under investigation,  $V$  is the container volume ( $0.035 \pm 0.003 \text{ m}^3$ ) and  $S$  is its surface ( $0.257 \pm 0.013 \text{ m}^2$ ).  $^{222}\text{Rn}$  takes too long to reach a threshold in one field day (Fig. 1c & 1d). Most  $^{220}\text{Rn}$  measurement series had a clear threshold phase (Fig. 1a), but some were unstable (Fig. 1b). Tipping points were identified through local regression (10% decrease in slope), and only thresholds lasting 6 min (1-min measurements) or 15 min (5-min measurements) were included when also mean and standard deviation were less than 22% of the tipping point value. 12 series ( $^{220}\text{Rn}$ ) were discarded (11 in year 2023).

The exhalation rate of Rn can also be estimated from the linear phase (25) as

$$\Phi = A \cdot \frac{V}{S} \quad \text{Eq. 3}$$

where  $A$  ( $\text{Bq m}^{-3} \text{ s}^{-1}$ ) is the slope of the activity concentration as a function of time determined by linear regression (R Core Team 2016). Here, we use the three first measurements after placement of the container, and to ascertain linearity, these must give an  $R^2$  of at least 0.80 (6 cases of 5-min measurements led to the inclusion of only two points).

We assess also an ISO alternative, including the reference activity measurement in the slope, using otherwise the same methodology to avoid using only two points. The inclusion of any measurements deviating from linearity towards threshold will reduce the slope (18), giving an under-bias of exhalation rate. The linear assessment can be improved by including the reference measurement, which should give a better estimate of the slope.

The inclusion of the reference measurement, in some cases, involved more than one potential slope. We, therefore, also assess the steepest possible slope using at least three measurement points, where the reference measurement may be included, using otherwise the same method as the ISO.

Finally, with the method of Seo et al. (18), we use non-linear least squares exponential fitting (R Core Team 2016) of both the linear increase and the threshold phases of  $^{220}\text{Rn}$  to estimate the exhalation rate:

$$\Phi = \frac{B \cdot k \cdot V}{S} \quad \text{Eq. 4}$$

where  $B = \frac{\Phi \cdot S}{V \cdot \lambda}$  ( $\text{Bq m}^{-3}$ ) and  $k = \lambda$  ( $\text{s}^{-1}$ ). Here, the reference measurement is included. Parameter estimations of  $B$  and  $k$  with a  $P$ -value higher than 0.1 were rejected. Due to fluctuations in the threshold, 7 (35%) exhalation rate estimates were discarded in 2023.

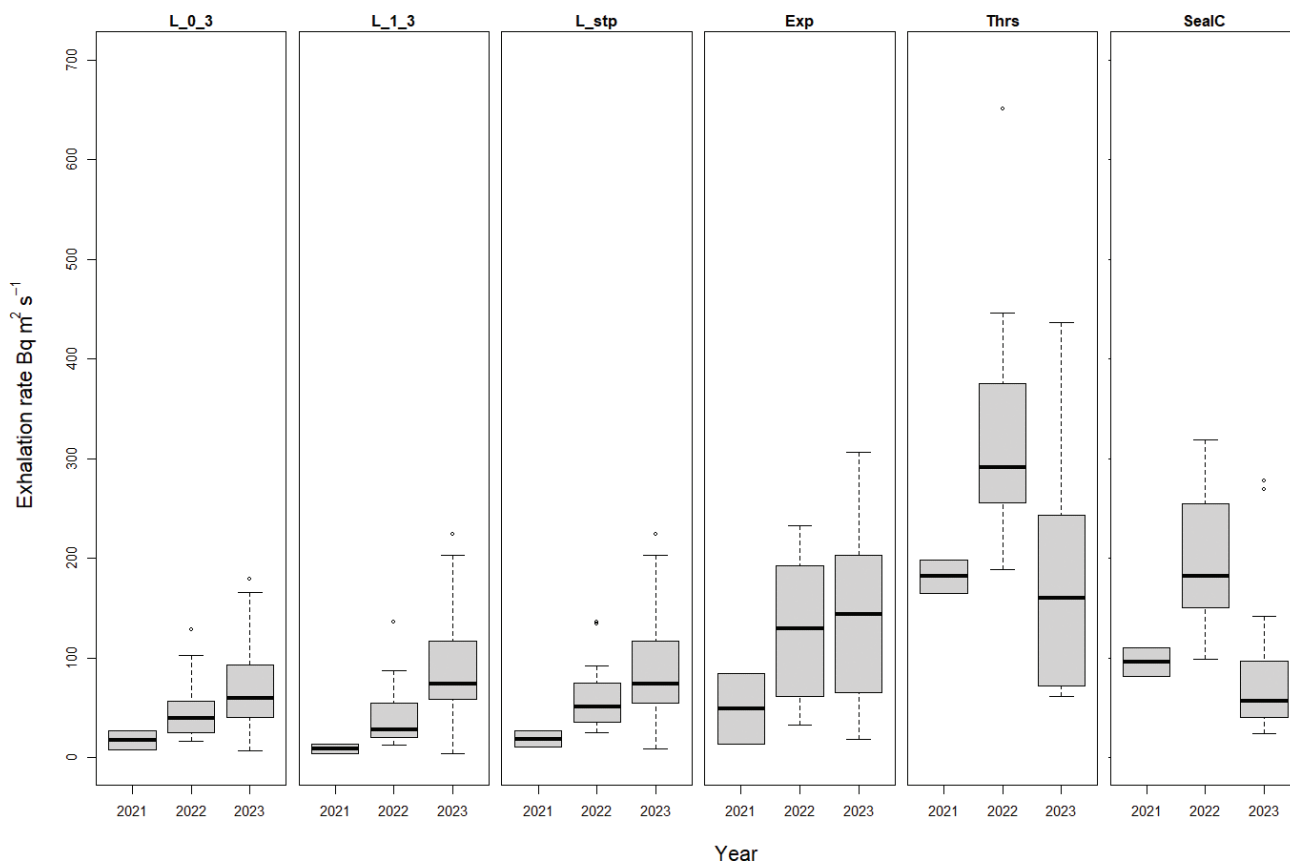


**Fig. 2.** Yearly exhalation rate of  $^{220}\text{Rn}$ , calculated using each of six methods: linear with reference measurement (L\_0\_3), linear ISO (L\_1\_3), steepest linear (L\_stp), exponential fitting (Exp), threshold (Thrs) and sealed-can (SealC).

On nine field days, soil gas Rn was measured (5-min) after exhalation using EQF and RTM1688-2 (SARAD®), with recommended airflow rates of 0.75 L/min and 0.3 L/min, respectively, and a DurrIDGE soil gas probe. For details, see the Supplementary material.

Weather data were downloaded from the Norwegian Meteorological Institute ([api.met.no](http://api.met.no)). This included 10-min data on temperature and air humidity from a nearby (1700 m) weather station (Ulefoss, SN32540) and hourly data for several parameters from another (Gvarv, SN32060, 12 km). There was a strong correlation in temperature ( $R = 0.965$ ,  $CI_R$ : 0.962–0.967) and humidity ( $R = 0.936$ ,  $CI_R$ : 0.931–0.949) between the two stations, supporting use of Ulefoss for 10-min and Gvarv for hourly data. Water drains from soil over several days (26, 27), so we included precipitation the last five prior days. Temperature, pressure and wind can affect exhalation and were included, in addition to air humidity, which can affect instruments.

There were too few exhalation rate estimates for  $^{222}\text{Rn}$  for any statistics. Due to different  $^{220}\text{Rn}$  exhalation between years (Fig. 2) and corresponding different uses of side versus top valve for sampling in 2021/2022 versus 2023, respectively, as well as different measurement

periods, being only 5-min in 2021, a mix in 2022 and only 1-min in 2023, these (termed valve and meas, respectively) were included as terms in linear models (R Core Team 2016). Then, we successively removed the most unlikely term until all terms were significant. This was done for each of the six methods of calculating exhalation rate, starting with the full statistical model:

$$\text{Exhal} \sim \text{Temp}_{\text{air}} + \text{Humid} + \text{Press} + \text{windspeed} + \text{windDIR} + \text{precip} + \text{meas} + \text{valve}$$

Models were compared through Akaike's Information Criterion (AIC) (28).

## Results

$^{222}\text{Rn}$  in soil gas ranged from 1,400 to 5,900  $\text{Bq m}^{-3}$  (mean: 3,600, SD: 1,600) and was correlated to its exhalation rate from soil ( $r = 0.78$ ,  $P > 0.07$ ), which ranged from 0.01 to 0.02  $\text{Bq m}^{-2} \text{s}^{-1}$  (mean: 0.17, SD: <0.01) for the two linear phase methods.  $^{220}\text{Rn}$  in soil gas ranged from 2,300,000 to 8,300,000  $\text{Bq m}^{-3}$  (mean: 6,100,000, SD: 2,000,000) and was only weakly and not significantly correlated to its exhalation rate ( $r = 0.1$ ,  $P > 0.09$ ), probably due to the short half-life of  $^{220}\text{Rn}$ . Using the six methods based on different phases of accumulation in

## Correlation between methods

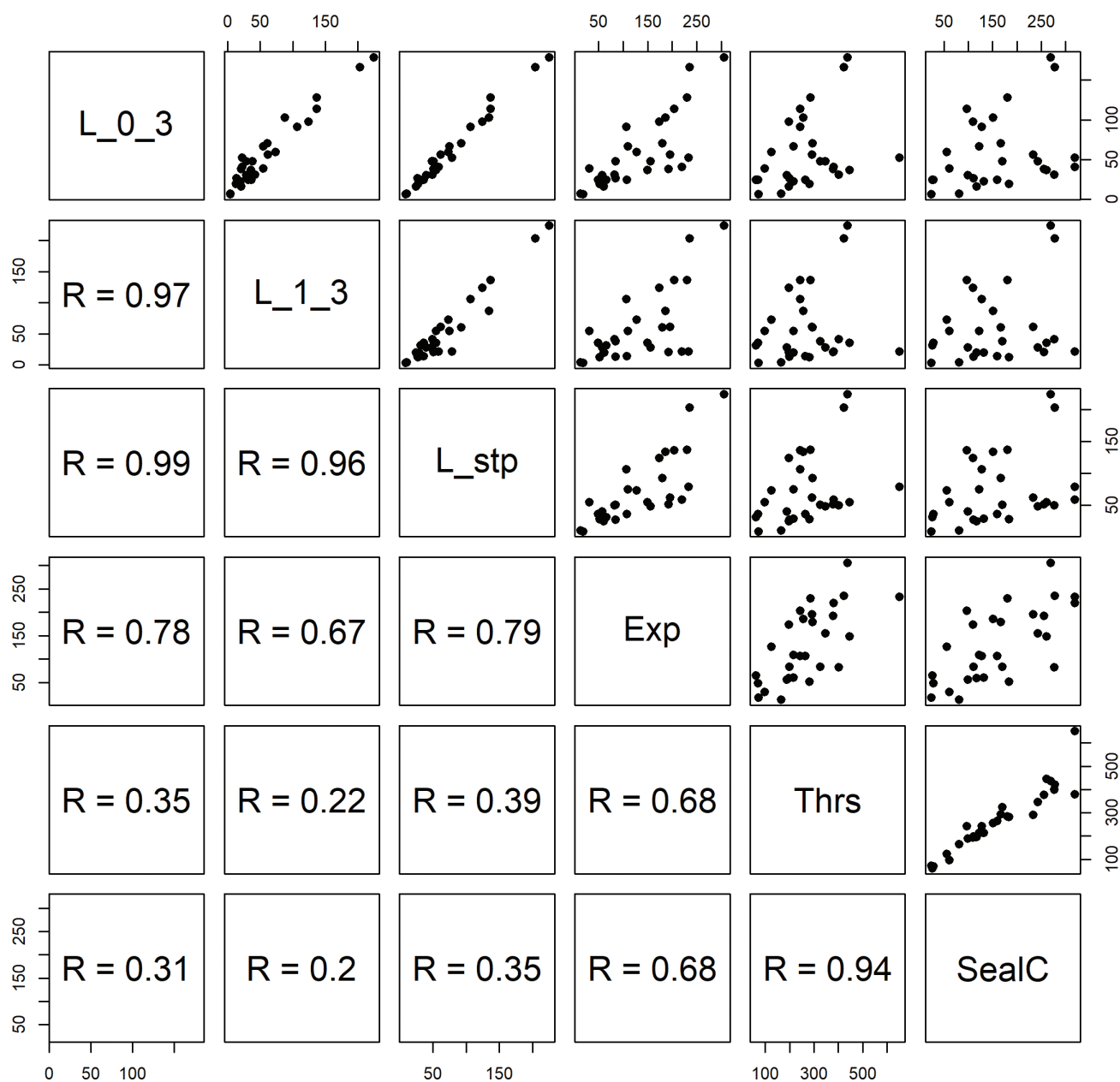


**Fig. 3.** Correlation plots (upper panel) and Pearson's coefficient (lower panel) between each of the six methods to calculate exhalation: linear with reference measurement (L\_0\_3), linear ISO (L\_1\_3), steepest linear (L\_stp), exponential fitting (Exp), threshold (Thrs) and sealed-can (SealC).

the container, across all field days and methods of calculation, the exhalation rate of  $^{220}\text{Rn}$  was high and varied from 3.5 to 650  $\text{Bq m}^2 \text{s}^{-1}$  at the Fen HBRA. For  $^{220}\text{Rn}$ , the three methods using only the linear phase were correlated, as were also the sealed-can and threshold phase methods (Fig. 3). There was large variation in exhalation rate both amongst and within methods (Fig. 4). The threshold method often gave the largest estimates, the

three linear phase methods the lowest and the sealed-can and exponential fitting methods were intermediate in value (Table 1 & Fig. 4). The largest simultaneous difference between methods (one series of exhalation measurements) was a 30 times difference of 630  $\text{Bq m}^2 \text{s}^{-1}$  for  $^{220}\text{Rn}$ , but on the two last field days, differences were small (less than 72  $\text{Bq m}^2 \text{s}^{-1}$ ). There was monthly and seasonal variation, as shown for the linear method

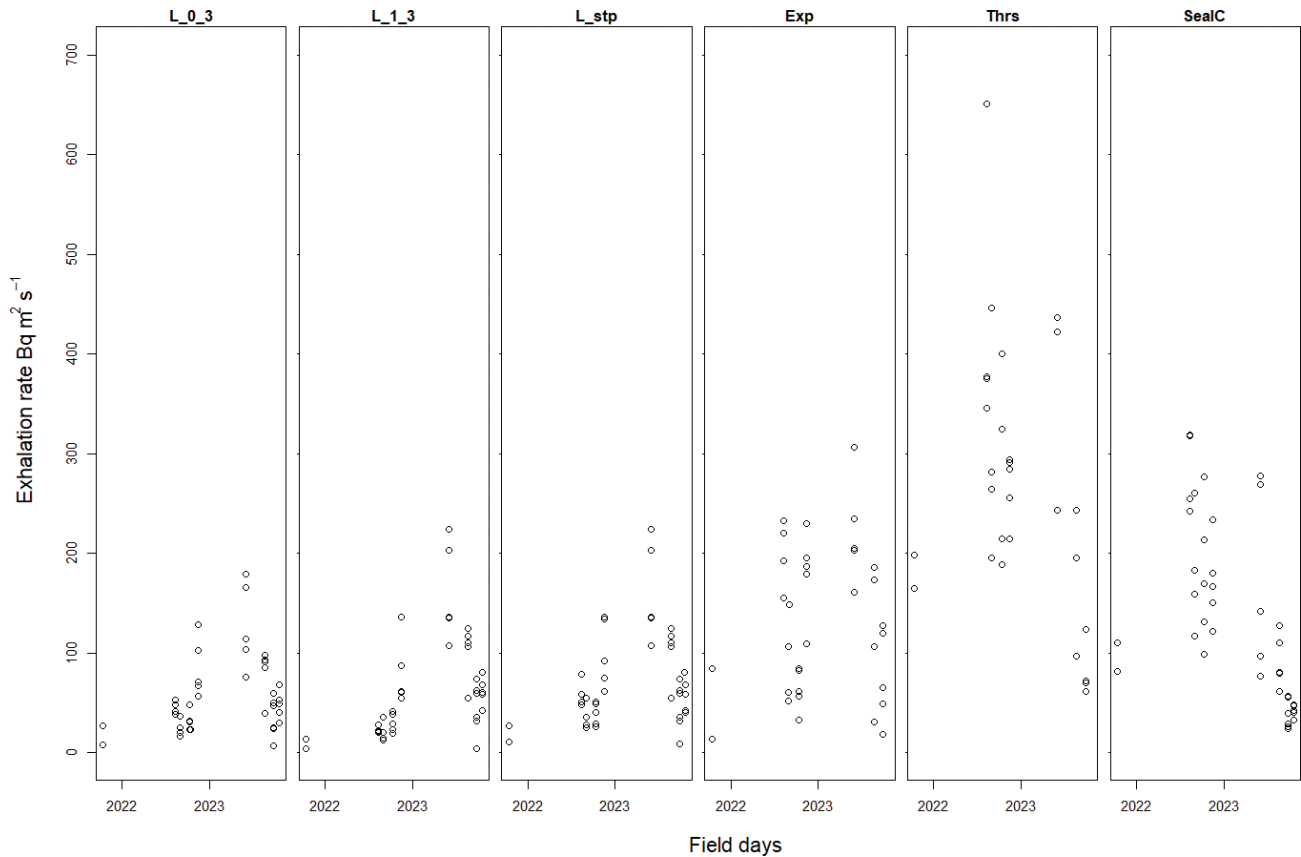


**Fig. 4.** Temporal exhalation rate of  $^{220}\text{Rn}$ , using each of the six methods: linear with reference measurement (L\_0\_3), linear ISO (L\_1\_3), steepest linear (L\_stp), exponential fitting (Exp), threshold (Thrs) and sealed-can (SealC).

**Table 1.** Exhalation rates calculated with each of the six different methods, minimum (min), maximum (max) and mean and variance (var): linear with reference measurement (L\_0\_3), linear ISO (L\_1\_3), steepest linear (L\_stp), exponential fitting (Exp), threshold (Thrs) and sealed-can (SealC)

Method	Min	Max	Mean	Var
L_0_3	6.5	180	58	1,600
L_1_3	3.5	220	64	2,700
L_stp	8.8	220	73	2,400
Exp	13	310	130	5,700
Thrs	62	650	270	18,000
SealC	24	320	140	7,800

including the reference measurement (Fig. 5), with higher exhalation in summer than spring/autumn.

Linear regression showed that variation in  $^{220}\text{Rn}$  exhalation rates could be explained by some weather parameters after model simplification (Table 2). The better AIC for exponential fitting and threshold methods are due to discarded data points related to shifts in the threshold and fewer degrees of freedom. These methods and linear

phase ISO explain more variation ( $R^2_{\text{adj}}$ ). The latter had the second strongest F-statistics, which was strongest for the steepest linear phase method. Looking to heteroscedasticity, leverage and residuals linearity, the linear phase method including reference point, the linear phase steepest and the exponential fitting seem best (Supplementary material 4).

Wind speed was significant for all six methods, either with the highest or second highest positive effect size (Table 2). Differences in wind speed (Fig. 6) could help explain the observed differences between years 2021/2022 and 2023. Temperature and precipitation were significant for most methods. Precipitation always had a negative impact, as expected from increased levels of soil moisture. Temperature in the linear phase ISO method had a negative impact, whilst in the three methods using threshold, had a positive effect. Also, for methods using the threshold phase, switching from using the exhalation container side valve to the top valve had a negative effect with the largest (or second largest) effect size. This suggests a heterogeneous distribution of  $^{220}\text{Rn}$  in the exhalation container, as diffusion

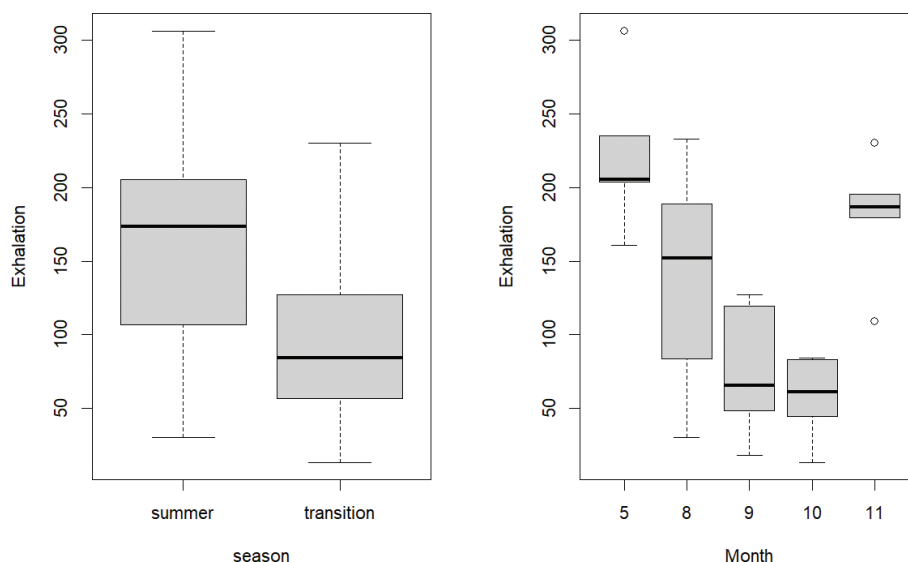


**Fig. 5.** Seasonal and monthly exhalation rates of  $^{220}\text{Rn}$  in the Fen complex, calculated using the linear increase phase including the reference measurement (L\_0\_3), the best model in the model selection.

speed and decay may involve lower levels under the roof. For the method using the linear phase with the reference measurement, the measurement period was significant with a negative effect. This can be expected when, measurements are few, and points after the linear phase deviating from linearity towards threshold are included (18).

### Discussion

In this study, we optimise methodology and demonstrate high exhalation rates of  $^{220}\text{Rn}$  in the HBRA Fen igneous complex. It is well known that health risks to  $^{222}\text{Rn}$  and  $^{220}\text{Rn}$  are increased in HBRAs (3, 4). Increased risk from various exposure scenarios has been shown for the Fen complex (5–8, 29–33). Levels of radon-progenitors in soil are high (6, 29, 32, 34), and there are high outdoor levels of  $^{220}\text{Rn}$  (6, 29, 32, 34). Natural ventilation from the Fen legacy iron mines has a large local impact on outdoor levels (8), and we show that  $^{220}\text{Rn}$  exhalation from the ground is also significant and should be taken into account when assessing outdoor exposure. Such an assessment requires knowledge about the magnitude and variation of exhalation from the ground. We demonstrate seasonal variation and effects of weather parameters. In summer, outdoor occupancy by the public is frequent, and  $^{220}\text{Rn}$  exhalation is highest, contributing most to outdoor levels and exposure.

Wind and precipitation were significant in all statistical models. All weather parameters could have had an effect (11), but there are too few data to incorporate enough variation for all parameters to become significant. Especially, linear phase methods of short-lived

$^{220}\text{Rn}$  are, with long measurement periods, prone to sparse datapoints and under-bias from inclusion of points after deviating from linearity. For  $^{222}\text{Rn}$ , on the other hand, due to the much longer duration of the linear phase, it takes too long to reach the threshold in one field day, and only one exhalation estimate is possible per field day. Moreover, results are probably affected by the large uncertainties. For  $^{220}\text{Rn}$ , the larger effect size of wind speed and different use of side versus top valve of the exhalation container suggest that these parameters are most important. They probably result from forced exhalation with wind and a heterogenous distribution with lower levels against the exhalation container roof, respectively. The latter involves violation of the assumption of a homogenous distribution and involves lower exhalation rate estimates for methods using the threshold when the top valve is used for sampling, as suggested by the negative effect size. This issue is probably most important for  $^{220}\text{Rn}$  due to its short half-life and dependence on distance to its source (2). Incidentally, it was also in the year 2023, when the top valve was used, that the majority of discarded exhalation rate estimates due to threshold instability were made. A homogenous distribution within the exhalation container may be achieved if a fan for mixing air is included within the container, a measure we therefore recommend for future exhalation studies of  $^{220}\text{Rn}$ .

A major finding is the different calculated  $^{220}\text{Rn}$  exhalation rates when using the linear phase compared to the threshold phase. Seo et al. (18) also found higher rates of exhalation with an exponential fitting method compared to the linear phase ISO method, even though not

**Table 2.** Estimates of significant parameters (standard error) in linear models of the six methods for exhalation rate variation in relation to air temperature (Temp), air humidity (Humid), atmospheric pressure (Press), wind speed (Wind), wind direction (Dir), one day precipitation (24hprecip), five days precipitation (5dayprecip), length of measurement interval (meas) and going from using side valve to top valve for sampling from exhalation container (Valve). The six methods: using linear phase and reference measurement (L\_0\_3), linear phase according to ISO (L\_1\_3), steepest linear (L\_stp), exponential fitting (Exp), threshold (Thrs), and sealed-can (SealC). For each model, adjusted R-squared (R2adj), F-statistics (F), degrees of freedom (df) and AIC given.

Method	Temp	Humid	Press	Wind	Dir	5dayP	Meas	Valve	R <sup>2</sup> adj	F	df	AIC
L_0_3				26(4.3)		-0.02(0.01)	-5.1(2.5)		0.64	24	37	383
L_1_3	-3.9(1.2)	-0.86(0.34)		41(4.4)					0.70	32	37	396
L_stp				37(4.3)		-0.02(0.01)			0.64	37	38	398
Exp	4.5(1.4)			73(12)	-0.38(0.12)	-0.04(0.02)		-69(28)	0.72	18	28	355
Thrs	12(2.3)			91(20)		-0.08(0.04)		-230(51)	0.76	23	24	331
SealC	8.3(1.7)		-4.1(2.2)	33(9.2)		-0.06(0.02)		-140(21)	0.74	24	35	436

as large as observed in our study. The decrease of this difference towards the end of the study is probably related to the effect of using the top valve on the threshold methods. Thus, going from using the side valve to the top valve of the container involved lower exhalation rates in 2023 for the threshold models (Fig. 2 and Table 2), which level out the difference between the linear phase and threshold methods. However, the effect size of wind speed was equal or stronger for the threshold methods, and higher wind speeds in the last study year may also have acted to reduce the difference. It is, therefore, not clear whether the identified difference between linear phase and threshold methods is real or only present if the side valve is used.

Nonetheless, threshold methods for <sup>220</sup>Rn are prone to fluctuations (Fig. 1b), and discarding these results in reduction of data. The linear methods provide a clear advantage, as shorter measurement series allow more data points in one day and better assessment of temporal variation. Inclusion of the reference measurement in a measurement series allows more data points, possibly avoiding deviations from linearity and a better estimate of the slope, which is important due to the short half-life <sup>220</sup>Rn. However, in areas where soil levels of radon-progenitors are much lower than in HBRA's like the Fen complex, the measurement period may need to be longer for measurements to be above the instruments' detection limit, which may hinder enough data points being collected during the linear phase. In such areas, for <sup>220</sup>Rn, the threshold or sealed-can method must be used.

This study is limited to one geographical point and few data due to time constraints and limited resources. Other locations should be assessed, and future studies should include more data to better assess effects from weather parameters and diurnal variation. Weather data representative of the local microclimate should be attained using a local portable weather station. To better assess outdoor levels of Rn isotopes in Fen to assess exposure and risk, more studies should be undertaken on spatial variation of soil exhalation and natural chimney ventilation from mine openings.

## Conclusions

Our results show a significant exhalation rate of <sup>220</sup>Rn from the ground in the Fen igneous complex, as expected, but with large temporal variations. Statistical modelling shows that this can be explained by weather parameters and, in particular, by wind speed. The use of the linear phase of accumulation gives lower estimates of exhalation rate than methods using the threshold phase. This difference is less pronounced if the top valve of the exhalation container is used for sampling air. For <sup>220</sup>Rn, it is important to use as short as possible measurement periods to attain enough measurement points during the linear phase.

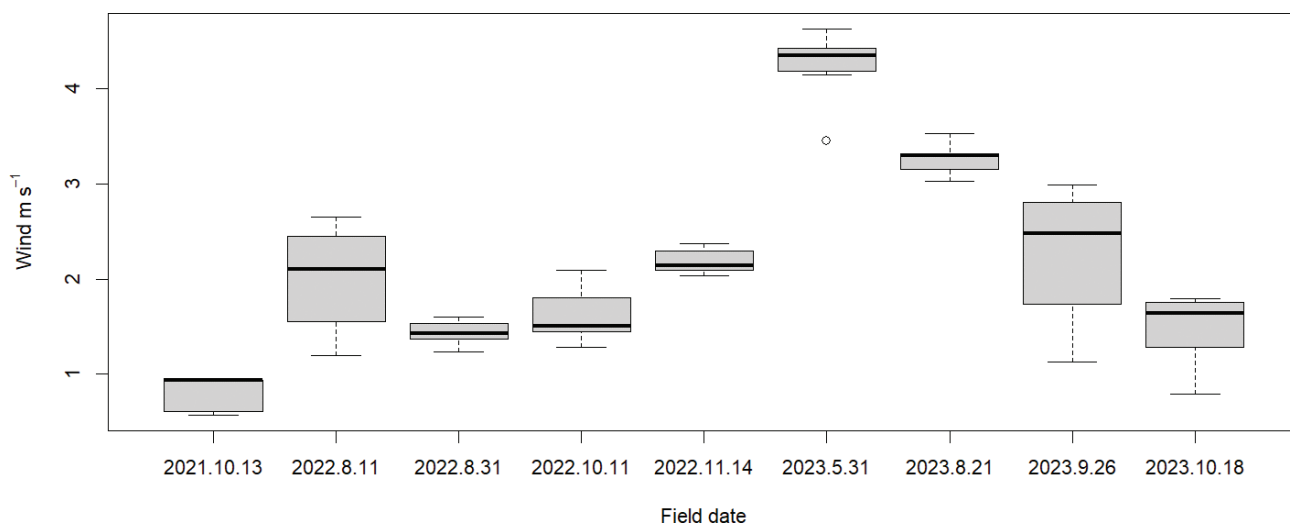


Fig. 6. Wind speed during the different field days at the Fen complex.

To attain more exhalation rate estimates, methods using the linear phase of accumulation should be used, if levels are high enough to attain enough measurements during the linear phase.

### Acknowledgements

This research was part of the RadoNorm project. This study received funding from the Euratom research and training programme 2019–2020 under grant agreement No 900009 from the Research Council of Norway (EU-STRA). We thank Justin E Brown at DSA for linguistic and grammar proofreading.

### References

- United Nations Scientific Committee on the Effect of Atomic Radiation (UNSCEAR). Exposures from natural radiation sources. Volume I, Annex B. UNSCEAR report to the General Assembly, with annexes. New York, NY: United Nations Scientific Committee on the Effect of Atomic Radiation; 2000.
- United Nations Scientific Committee on the Effect of Atomic Radiation (UNSCEAR). Effects of ionizing radiation. Volume II, Annex E. UNSCEAR report to the General Assembly, with annexes. New York, NY: United Nations Scientific Committee on the Effect of Atomic Radiation; 2006.
- Aliyu AS, Ramli AT. The world's high background natural radiation areas (HBNRAs) revisited: a broad overview of the dosimetric, epidemiological and radiobiological issues. *Radiat Meas* 2015; 73: 51–9. doi: 10.1016/j.radmeas.2015.01.007
- Sohrabi M. World high background natural radiation areas: need to protect public from radiation exposure. *Radiat Meas* 2013; 50: 166–71. doi: 10.1016/j.radmeas.2012.03.011
- Stranden E. The radiological impact of mining in a Th-rich Norwegian area. *Health Phys* 1985; 48: 4. doi: 10.1097/00004032-198504000-00003
- Popic JM, Bhatt CR, Salbu B, Skipperud L. Outdoor  $^{220}\text{Rn}$ ,  $^{222}\text{Rn}$  and terrestrial gamma radiation levels: investigation study in the thorium rich Fen Complex, Norway. *J Environ Monit* 2012; 14: 1. doi: 10.1039/c1em10726g
- Haanes H, Skjerdal HK, Mishra R, Rudjord AL. Outdoor measurements of thoron progeny in a  $^{232}\text{Th}$ -rich area with deposition-based alpha track detectors and corrections for wind bias. *J Eur Radon Assoc* 2021; 2: 6130. doi: 10.35815/radon.v2.6130
- Haanes H, Rudjord AL. Significance of seasonal outdoor releases of thoron from airflow through a point source during natural ventilation of a mine-complex in thorium-rich bedrock. *Atmos Pollut Res* 2018; 9: 6. doi: 10.1016/j.apr.2018.03.007
- Tanner AB. Radon migration in the ground: a supplementary review. In: Gesell TF, Lowder WM, eds. *Natural radiation environment III*. Vol 1. CONF-780422. Washington, DC: U.S. Department of Energy; 1980, pp. 5–56.
- Nazaroff WW. Radon transport from soil to air. *Rev Geophys* 1992; 30(2): 137–60. doi: 10.1029/92RG00055
- Porstendörfer J. Properties and behaviour of radon and thoron and their decay products in the air. *J Aerosol Sci* 1994; 25(2): 219–63. doi: 10.1016/0021-8502(94)90077-9
- Tanner AB. Radon migration in the ground: a review. In: Adams JAS, Lowder WM, eds. *The natural radiation environment*. Chicago, IL: University of Chicago Press; 1964, pp. 161–90.
- Abodunrin OP, Akinloye MK. Determination of radon exhalation rates from soil around buildings in Lagos environments using passive measurement technique. *J Environ Health Sci Eng* 2020; 18(1): 129–35. doi: 10.1007/s40201-020-00446-3
- Kaliprasad CS, Vinutha PR, Narayana Y. Natural radionuclides and radon exhalation rate in the soils of Cauvery River Basin. *Air Soil Water Res* 2017; 10: 1178622117746948. doi: 10.1177/1178622117746948
- Thabayneh KM. Determination of radon exhalation rates in soil samples using sealed can technique and CR-39 detectors. *J Environ Health Sci Eng* 2018; 16(2): 121–8. doi: 10.1007/s40201-018-0298-2
- Hafez AF, Moharram BM, El-Khatib AM, Abdel-Naby A. Effective radium content in Egyptian soil by CR-39 and LR-115 plastic nuclear track detectors. *Isot Environ Health Stud* 1991; 27(4): 185–8. doi: 10.1080/10256019108622504
- Mazur J, Kozak K. Complementary system for long term measurements of radon exhalation rate from soil. *Rev Sci Instrum* 2014; 85: 022104. doi: 10.1063/1.4865156
- Seo J, Nirwono MM, Park SJ, Lee SH. Standard measurement procedure for soil radon exhalation rate and its

- uncertainty. *J Radiat Prot Res* 2018; 43(1): 29–38. doi: 10.14407/jrpr.2018.43.1.29
19. de Martino S, Sabbarese C, Monetti G. Radon emanation and exhalation rates from soils measured with an electrostatic collector. *Appl Radiat Isot* 1998; 49(4): 407–13. doi: 10.1016/S0969-8043(96)00300-4
  20. Popic JM, Meland S, Salbu B, Skipperud L. Mobility of radionuclides and trace elements in soil from legacy NORM and undisturbed naturally <sup>232</sup>Th-rich sites. *Environ Sci Process Impacts* 2014; 16(5): 1124–34. doi: 10.1039/c3em00569k
  21. Sharma N, Virk HS. Exhalation rate study of radon/thoron in some building materials. *Radiat Meas* 2001; 34(1): 467–9. doi: 10.1016/S1350-4487(01)00208-6
  22. de With G, Kovács T, Csordás A, Tschiersch J, Yang J, Sadler SW, et al. Intercomparison on the measurement of the thoron exhalation rate from building materials. *J Environ Radioact* 2021; 228: 106510. doi: 10.1016/j.jenvrad.2020.106510
  23. Jamir S, Sahoo B, Mishra R, Bhomick P, Sinha D. A study on indoor radon, thoron and their progeny level in Mokokchung district of Nagaland, India. *J Radioanal Nucl Chem* 2021; 331: 21–30. doi: 10.1007/s10967-021-08096-x
  24. Bonczyk M, Chałupnik S, Wysocka M, Grygier A, Hildebrandt R, Tosheva Z. The determination of radon/thoron exhalation rate in an underground coal mine-preliminary results. *Int J Environ Res Public Health* 2022; 19(10): 6038. doi: 10.3390/ijerph19106038
  25. ISO IOFS. Measurement of radioactivity in the environment – air: radon-222. Part 7 – accumulation method for estimating surface exhalation rate. International Organization for Standardization, Geneva, CH. ISO 11665-7:20122012. pp. 1–22.
  26. Buyuktas D, Bastug R, Aydinsakir K. Evaluating drainage design parameters by numerical experimentation. *Akdeniz Univ Ziraat Fak Derg* 2010; 23: 151–6.
  27. Romano N, Santini A. Water retention and storage: field. 2002, in Dane JH, Topp GC, eds. *Methods of Soil Analysis*. Soil science society of America, Madison. pp. 721–38.
  28. Burnham KP, Anderson DR. Model selection and multimodel inference. A practical information-theoretic approach. 2nd ed. Berlin: Springer; 2002.
  29. Popic JM, Salbu B, Strand T, Skipperud L. Assessment of radionuclide and metal contamination in a thorium rich area in Norway. *J Environ Monitor* 2011; 13(6): 1730–8. doi: 10.1039/c1em10107b
  30. Stranden E, Strand T. Natural gamma radiation in a Norwegian area rich in Thorium. *Radiat Protect Dosimetry* 1986; 16(4): 325–8. doi: 10.1093/oxfordjournals.rpd.a079765
  31. Haanes H, Dahlgren S, Rudjord AL. Cold season dose rate contributions from gamma, radon, thoron or progeny in legacy mines with high natural background radiation. *Radiat Protect Dosimetry* 2023; 199(12): 1284–94. doi: 10.1093/rpd/ncad178
  32. Haanes H, Finne IE, Kolstad T, Mauring A, Dahlgren S, Rudjord AL. Outdoor thoron and progeny in a thorium rich area with old decommissioned mines and waste rock. *J Environ Radioact* 2016; 162–163: 23–32. doi: 10.1016/j.jenvrad.2016.05.005
  33. Haanes H, Finne IE, Skjerdal HK, Rudjord AL. Indoor and outdoor exposure to radon, thoron and thoron decay products in a NORM area with highly elevated bedrock thorium and legacy mines. *Radiat Res* 2019; 192(4): 431–9. doi: 10.1667/RR15403.1
  34. Haanes H, Gjelsvik R. Reduced soil fauna decomposition in a high background radiation area. *PLoS One* 2021; 16(3): e0247793. doi: 10.1371/journal.pone.0247793

---

**\*Hallvard Haanes**

Norwegian Radiation and Nuclear Safety Authority  
 P.O. Box 55, 1332 Østerås, Norway  
 Email: Hallvard.Haanes@dsa.no